eman ta zabal zazu

Universidad del País Vasco Euskal Herriko Unibertsitatea

Universidad del País Vasco/Euskal Herriko Unibertsitatea/ University of the Basque Country

Faculty of Chemistry

Degree of Chemistry

BACHELOR'S DEGREE FINAL PROJECT

"Synthesis of crosslinked polymers with reversible enamine-type bonds."

Author: Marta Aldecoa Ortueta

Supervisors: Josetxo Pomposo and Fabienne Barroso

San Sebastián, June 2023

Universidad del País Vasco Euskal Herriko Unibertsitatea

INDEX

ABSTRACT:

Polyglycidol-based crosslinked networks have emerged as a promising type of materials with diverse applications due to their unique chemical structure and tuneable properties. Polyglycidol, a hydrophilic polymer derived from glycidol monomers, possesses a high number of hydroxyl groups along its backbone, enabling it to form strong and versatile networks through crosslinking reactions.

In this work, cyclic branched polyglycidol was synthetized by zwitterionic ring-opening polymerization and then functionalized with *tert*-butyl acetoacetate in order to subsequently synthetize polyglycidol-based crosslinked networks. This was achieved by using 1,3-diaminopropane (DAP) as a crosslinker. Samples were synthetized with different amounts of DAP relative to the amounts of acetoacetate groups in the functionalized polymer in order to study their glass transition temperature (Tg), showing a maximum Tg value around 140 °C. In addition, all of the obtained samples have shown thermal stability up to 200 °C. Finally, the generated enamine`s bond ability to exchange with other amines was tested, as well as the pH-responsiveness of the obtained crosslinked networks.

The obtained materials were characterized by Fourier Transform Infrared Spectroscopy (FTIR), Differential Scanning Calorimetry (DSC), Thermogravimetric Analysis (TGA), Nuclear Magnetic Resonance (NMR), Gel Permeation Chromatography (GPC) and Elemental Analysis (EA)

RESUMEN:

Las redes entrecruzadas basadas en polyglicidol se han convertido en un prometedor tipo de materiales con diversas aplicaciones debido a su estructura química única y propiedades ajustables. El polyglicidol, un polímero hidrofílico derivado de monómeros de glycidol, posee un alto número de grupos hidroxilo a lo largo de su estructura principal, lo que le permite formar redes fuertes y versátiles a través de reacciones de entrecruzamiento.

En este trabajo, se sintetizó polyglicidol ramificado cíclico mediante una polimerización por apertura de anillo zwitterionica y luego se funcionalizó con *tert*-butyl acetoacetato para posteriormente sintetizar redes poliméricas basadas en glycidol. Esto se logró empleando 1,3-diaminopropane (DAP) como entrecruzante. Las muestras fueron sintetizadas con diferentes cantidades de DAP respecto al número de grupos de acetoacetato en el polímero funcionalizado, con el objetivo de estudiar su temperatura de transición vítrea (Tg), obteniendo un valor máximo de Tg cercano a los 140 °C. Además, todas las muestras obtenidas mostraron estabilidad térmica hasta los 200 °C. Finalmente se estudió la habilidad de intercambio del enlace enamina con otras aminas, así como la sensibilidad al pH de las redes entrecruzadas obtenidas.

Los materiales obtenidos se caracterizaron mediante Espectroscopía Infrarroja por Transformada de Fourier (FTIR), Calorimetría Diferencial de Barrido (DSC), Análisis Termogravimétrico (TGA), Resonancia Magnética Nuclear (NMR), Cromatografía de Permeación en Gel (GPC) y Análisis Elemental (EA).

LABURPENA:

Polyglizidolean oinarritutako sare gurutzatuak hainbat aplikazio dituzten etorkizun handiko material bihurtu dira haien egitura kimiko berdingabeagatik eta propietate doigarriengatik. Polyglizidoak, hots, glycidol monomeroetatik eratorritako polimero hidrofilikoak, hidroxilo talde kopuru handia du bere egitura nagusian zehar, eta horrek sare indartsu eta aldakorrak sortzea ahalbidetzen dio elkar gurutzatzeko erreakzioen bidez.

Lan honetan, polyclizidol adarkatu ziklikoa sintetizatu zen eraztun zwitterionikoaren irekiearen bidezko polimerizazio baten bidez. Ondoren, *tert*-butyl azetoazetatorekin funtzionalizatu egin zen glyzidolean oinarritutako sare polimerikoak sintetizatzeko. Hori lortu ahal izateko, 1,3-diaminopropane (DAP) erabili zen gurutzatzaile gisa. Laginak DAP kantitate ezberdinekin sintetizatu ziren, polimero funtzionalizatuko azetoazetato taldeen kopuruarekiko, haien beirazko trantsizioaren tenperatura (Tg) aztertzeko helburuarekin eta 140 °C inguruko Tg-ko balio maximoa lortuz. Gainera, lortutako lagin guztiek egonkortasun termikoa erakutsi zuten 200 °C-ko tenperaturara arte. Azkenik, enamina lotura beste amina batzuekin trukatzeko trebetasuna aztertu zen, baita lortutako sare gurutzatuen pHarekiko sentikortasuna ere.

Lortutako materialak Espektroskopia infragorriaren Fourier transformazioa (FTIR), Ekorketako Kalorimetria Diferentzia (DSC), Analisi Termograbimetrikoa (TGA), Erresonantzia Magnetiko Nuklearra (NMR), Gel-iragazkortasunezko Kromatografia (GPC) eta Oinarrizko Analisiaren bidez (EA) bereizi dira.

1. INTRODUCTION:

1.1 Polymer definition:

Polymers are large molecules composed of repeating subunits called monomers. They are formed through a process called polymerization, where the monomers are chemically bonded together to create long chains or networks. These versatile polymeric materials play a crucial role in numerous applications for diverse industries, including plastics, textiles, adhesives, coatings, and many others **(Figure 1)**.

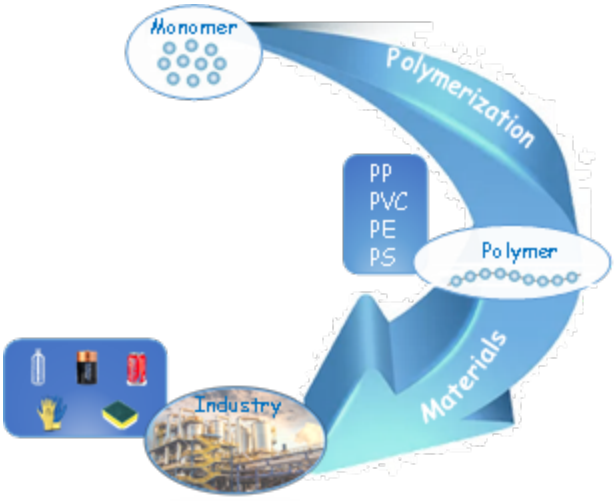

Figure 1: Scheme of monomer to polymer transformation and subsequent evolution towards an industrial material.

They exhibit a wide range of properties, such as flexibility, durability, thermal resistance, electrical insulation, and chemical resistance, which make them versatile and valuable in several fields. The properties of polymers are influenced by factors such as the chemical composition of the monomers, the polymerization process to obtain them, their molecular weight or the presence of fillers or additives. Specifically, polymers can be tailored for specific requirements in different applications by modifying these factors.

Polyethylene (PE), polypropylene (PP), polystyrene (PS), polyvinyl chloride (PVC), polyethylene terephthalate (PET) and many others are common examples of polymers. These materials find extensive use in everyday items like plastic bottles, packaging materials, clothing fibbers, automotive components and devices for energy storage.

1.2 Polymer classification:

Given the versatility of polymers, their classification can be done considering different criteria, including their chemical structure (**Figure 2**), physical properties or applications. Some common classification methods for polymers are summarized below:

- ### Based on monomer type

a) *Homopolymers* are composed of a single type of monomer or repeating unit. For example, polyethylene is a homopolymer of ethylene.

b) *Copolymers* are composed of two or more different types of monomers. Copolymers can be further classified into:

- Random copolymers: monomers are arranged randomly within the polymer chain.

- Block copolymers: monomers are grouped in blocks along the polymer chain.

- Graft copolymers: side chains of one monomer are attached to the main chain of another monomer.

- ### Based on polymer structure:

a) *Linear polymers* have a simple linear chain structure. Examples include high-density polyethylene (HDPE) and polyvinyl chloride (PVC).

b) *Branched polymers* have side branches or chains attached to the main polymer chain. Examples include low-density polyethylene (LDPE) and dendrimers.

c) *Crosslinked polymers (networks)* have a network-like structure due to the formation of covalent bonds between polymer chains. Examples include vulcanized rubber and thermosetting plastics. [1]

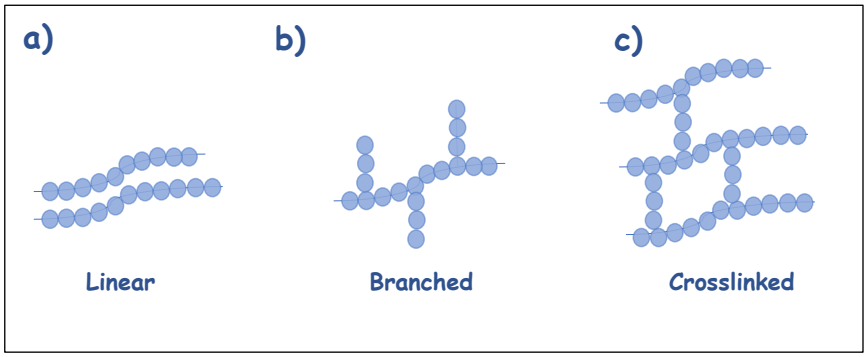

Figure 2: Classification of polymers depending on their structure.

- Based on physical properties:

a) *Thermoplastics* can be melted and re-molded multiple times without undergoing significant degradation. Examples include polyethylene, polypropylene, and polystyrene.

b) *Thermosetting plastics* undergo a permanent chemical change upon curing and cannot be re-melted or re-molded. Examples include epoxy resins and phenolic resins.

c) *Elastomers* exhibit elastic properties, meaning they can stretch and return to their original shape. Examples include natural rubber and synthetic elastomers like neoprene and silicone.

- Based on polymerization mechanism

a) *Addition polymers* are formed by the addition of monomers without the elimination of any by-products. Examples include polyethylene, polypropylene, and polystyrene.

b) *Condensation polymers* are formed by the elimination of small molecules, such as water or alcohol, during polymerization. Examples include polyesters, polyamides (nylons), and polyurethanes.

It is important to note that these manners to classify polymers are not mutually exclusive, and polymers can fall into multiple categories depending on their characteristics.

1.3 Ring Opening Polymerization

Particularly, the precursor cyclic polymers of this work were prepared using Zwitterionic Ring Opening Polymerization (ZROP), which is a type of organocatalyzed ring-opening polymerization. In the following sections, Ring Opening Polymerization (ROP) as well as ZROP will be introduced and briefly explained:

ROP is a type of polymerization reaction in which a cyclic monomer undergoes cleavage of the ring structure to form a linear polymer chain. This process involves the opening of a strained ring and the subsequent addition of monomers to the growing chain.

During ROP, a monomer with a cyclic structure, such as lactones, lactides, cyclic carbonates, or cyclic ethers, reacts with an initiator or a catalyst to initiate the polymerization reaction. The initiator or catalyst provides an active site or reactive species that can attack the cyclic monomer, leading to the opening of the ring and the formation of an active chain end. [2,3]

There are two main types of ROP mechanisms: *cationic* and *anionic*.

a) *Cationic* Ring-Opening Polymerization (CROP):

In CROP, an initiator or catalyst generates a positively charged species. Typical examples of initiators are Lewis acids and protonic acids. The positively charged generated species attacks the electron-rich site in the cyclic monomer, leading to the formation of a new cationic center. The polymer chain grows as monomers continue to add to the active cationic center, resulting in a longer polymer chain.
Examples of monomers that can undergo CROP include cyclic ethers, such as epoxides (e.g. ethylene oxide), cyclic acetals and cyclic carbonates.

b) *Anionic* Ring-Opening Polymerization (AROP):

In AROP, an initiator or catalyst generates a negatively charged species. This species reacts with the electron-poor site in the cyclic monomer, causing the ring to open and forming a new anionic center. Subsequent monomer additions occur at this active site, leading to chain growth.

Monomers that can undergo AROP polymerization include lactones (e.g. caprolactone), lactides, cyclic carbonates (e.g. trimethylene carbonate) and cyclic siloxanes (e.g. cyclic siloxanes).

ROP offers several advantages if you compare it with other types of polymerization processes. It can produce polymers with controlled molecular weights, low polydispersity, and well-defined end groups. It also enables to prepare polymers with unique properties such as biodegradability, shape-memory behaviour and controlled crystallinity. Furthermore, it is a versatile method of polymerization for synthesizing a wide range of polymers with diverse structures and properties to be used in several fields including materials science, biomedical engineering, and drug delivery systems. [4,5]

Besides, ZROP has emerged as an alternative approach, to facilitate the controlled and efficient polymerization of cyclic monomers and generate cyclic polymers.

ZROP is a type of chain polymerization where a growing macromolecule carries two ionic chain carriers with opposite charges at its ends. Usually, the polymerization starts from one of these ends. This technique involves a cyclic monomer and an initiator, that can be nucleophilic or electrophilic depending on its nature. Throughout the reaction and with the contribution of a catalyst, a propagating zwitterionic species is generated, wherein the chain ends interact electrostatically resulting in the formation of different rings based on their nature. During propagation, the monomer is consumed, and cyclization occurs due to the neutralization of charges at the chain ends, leading to the formation of a cyclic polymer. An example of ZROP with a nucleophilic catalyst (NZROP) involves the reactions of lactones with N-heterocyclic carbenes. [6] An example

of ZROP with an electrophilic catalyst (EZROP), as it has been displayed in this study, is the reaction of glycidol with tris(pentafluorophenyl)borane ($B(C_5F_6)_3$). [7]

In the specific case of glycidol, both the oxygen contained in the epoxide as well as the oxygen from the hydroxyl group are able to react with the $B(C_5F_6)_3$, allowing initiation in two different ways, as shown in **Figure 3**.

If initiation occurs through attack to the epoxide oxygen, the resulting species is represented in pathway (a), while if attack occurs to the hydroxyl group, the resulting species is represented in pathway (b). Regardless of the type of attack, the outcome is an oxonium ion, which is prone to be attacked by another monomeric unit during propagation.

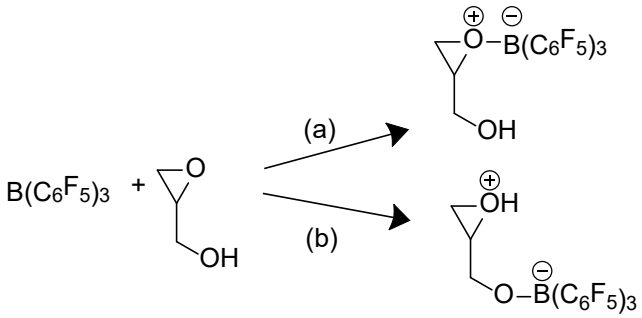

Figure 3: Initiation mechanism for the EZROP of glycidol with $B(C_6F_5)_3$. [8]

In the propagation reaction (**Figure 4**), the ring opening can occur competitively by attack of the monomer to both formed oxonium ions, leading to two different mechanisms.

The attack to the epoxide oxygen follows the Active Chain-End Mechanism (ACEM) and results in a repetitive unit of the $L_{1,3}$ type. When the attack is directed from the hydroxyl group, the mechanism is known as Activated Monomer Mechanism (AMM), leading to the $L_{1,4}$ structure. Consequently, a chain with a mixture of $L_{1,3}$ and $L_{1,4}$ structures is obtained, and the specific combination will depend on the kinetics followed by each mechanism.

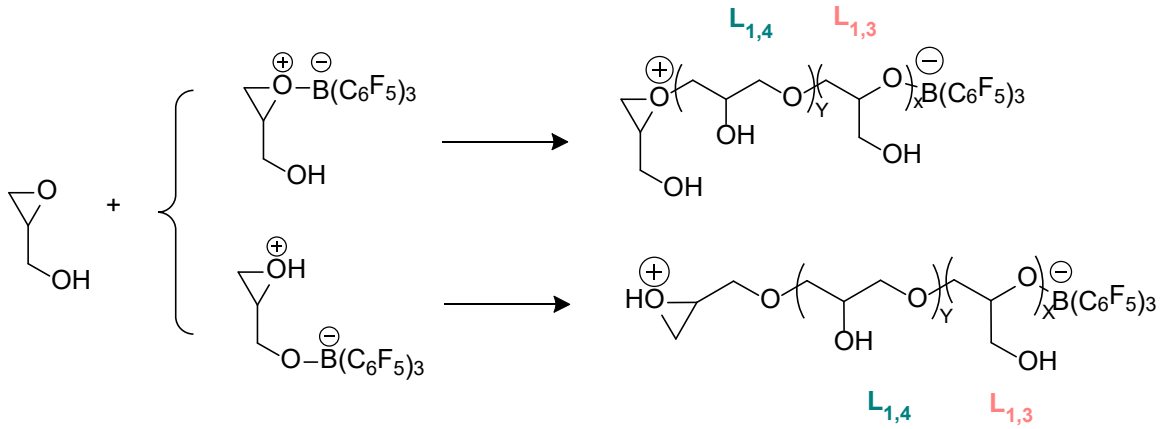

Figure 4: Propagation mechanism for the EZROP of glycidol with $B(C_6F_5)_3$. [8]

Finally, termination (**Figure 5**) occurs when there is neutralization of charges at the end of the chain that leads to the formation of cyclic structures. It has to be remarqued that the hydroxyl groups of the chains also react giving rise to branched structures. Because of these branching reactions, the final structure of the polymer is a cyclic-core surrounded by branches.

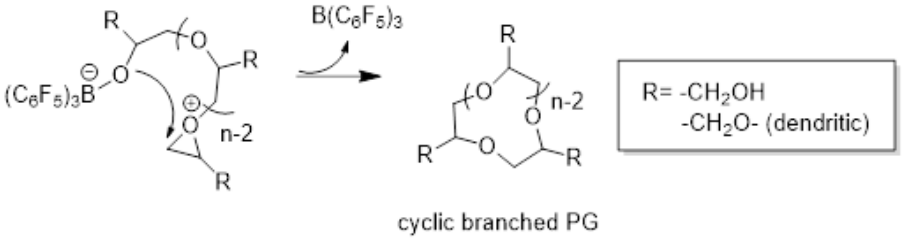

Figure 5: Termination mechanism for the EZROP of glycidol with $B(C_6F_5)_3$. [8]

1.4 Covalent Adaptable Networks:

Covalent Adaptable Networks (CANs) are defined as network structures that possess a sufficient number and arrangement of reversible covalent bonds. These bonds enable the cross-linked network to undergo chemical responses when exposed to an applied stimulus. Typically, the response involves changes in the stress and/or shape (strain) of the material, and it occurs without the material undergoing any irreversible degradation of the network structure, because of the maintenance of the initial bond density while the material is rearranging itself in response to the stimulus. This unique property makes CANs "smart" materials capable of dynamically responding to stimuli by altering their physical structure, state, and/or shape. [9-10]

According to the reaction mechanism, CANs can be further classified in associative and dissociative (**Figure 6**):

1. **Dissociative CANs:** The covalent bonds within the network undergo cleavage, resulting in reduced connectivity or even complete depolymerization. The broken bonds are then reformed in different positions, allowing structural rearrangement and dynamic changes in the material

2. **Associative CANs:** They are also commonly referred as “vitrimers”. Instead of bond cleavage, vitrimers rely on bond exchange while maintaining the network’s connectivity. This allows the crosslink density of the network to remain constant throughout the process, preserving its structural integrity. Initially, vitrimers were developed based on transesterification reactions, but over time, various other dynamic covalent associative bonds have been introduced. [11]

Nevertheless, it can be challenging to clearly distinguish the frontier between associative and dissociative mechanisms, as boundary between them is not always well-defined.

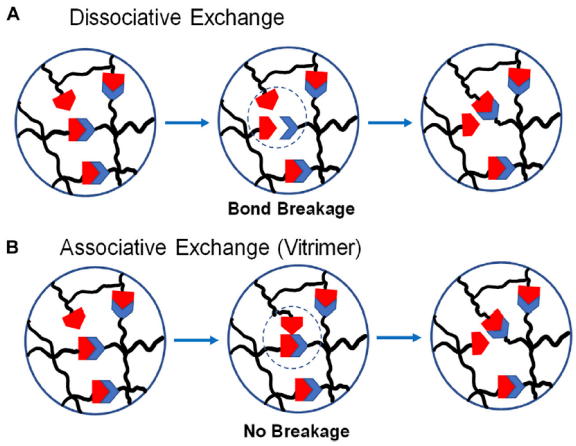

Figure 6: Covalent **adaptable** networks undergoing dynamic bond exchanges with (A) dissociative and (B) associative mechanisms. [12]

In essence, CANs are designed to exhibit adaptive behaviour without suffering permanent damage. By incorporating reversible covalent bonds, they can undergo controlled chemical responses to external influences, offering potential applications in diverse fields such as biomedical engineering, robotics, and materials science.

The functionalization of polyglycidol (PG) to form covalent networks in the form of CANs is a promising approach in the field of adaptable polymeric materials. PG is a polymer that contains reactive hydroxyl groups in its structure and its functionalization involves the introduction of specific functional groups into its polymer chains. Such functional groups can be selected to enable dynamic and reversible covalent chemical reactions. Once these functional groups are introduced, PG can form covalent networks through cross-linking reactions.

In the context of CANs, the functional groups in PG play a crucial role in the material's molecular adaptability. These functional groups can undergo reversible chemical reactions such as cyclization, hydrolysis, or transesterification. In this way, the reaction allows the formation and breakage of selective covalent bonds in the polymer network, resulting in changes in the structure and properties of the material.

Functionalization of PG to form covalent networks in the form of CANs offers several advantages. Firstly, it allows for adjustable molecular adaptability as the functional

groups can be designed to respond to specific stimuli such as temperature, pH, or light. This results in controllable changes in material properties such as stiffness, elasticity, and strength. Furthermore, the functionalization of PG can provide desirable features to CANs, such as self-repairing capabilities. The dynamic covalent bonds in the polymer network can break and reform in response to damage or defects, enabling the material to undergo self-healing without external intervention.

The advantages of PG synthetized by ZROP are that it can be produced in one-pot reaction, large-scale synthesis and the possibility to tune the topology. Therefore, in the present work, crosslinked networks will be obtained from PG synthetized by ZROP. In future works, crosslinked polymers based on PG with linear structure will be generated to be compared with the cyclic ones.

1.5 Reversible Enamine Bonds:

The enamine bond [13,14] belongs to the family of imine and hydrazone dynamic covalent bonds. [15] It was introduced as a "forgotten" dynamic covalent bond in polymer chemistry for the introduction of exchangeable and reversible links by Sanchez-Sanchez, Fulton and Pomposo in 2014. [16] Illustration of the dynamic nature of enamine bonds with model low molecular weight compounds containing ß-ketoester and amine functional groups is shown in **Figure 7**.

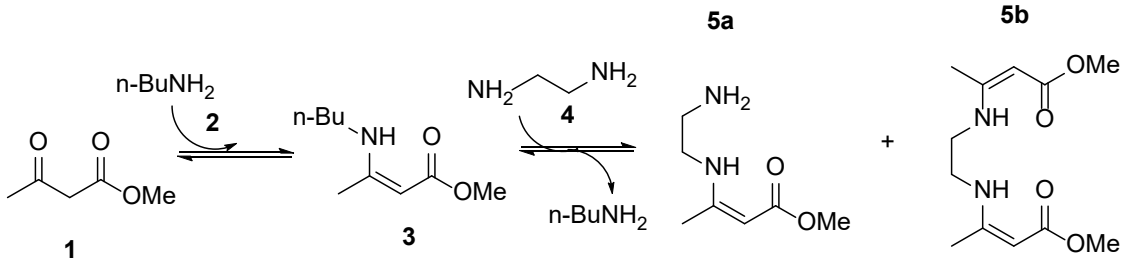

Figure 7: Illustration of the dynamic nature of enamine bonds: formation of an enamine (**3**) from the condensation of methyl acetoacetate (**1**) and n-butylamine (**2**), and its component exchange reaction with ethylenediamine (**4**) to form a bis-enamine (**5b**).

2. MOTIVATION AND GOALS:

The main goal of this work is to develop a synthetic procedure that allows generating polymeric networks based on branched cyclic polyglycidol through enamine type dynamic bonds.

To this aim, we will focus on the following partial objectives:

- Synthesis and characterization of polyglycidol.
- Functionalization of polyglycidol with *tert*-butyl acetoacetate (TBAA) and subsequent characterization of the compound.
- Synthesis of polymer networks with 1,3-diaminopropane (DAP) as a crosslinker.
- Thermal characterization and spectroscopic characterization of polyglycidol-based crosslinked networks.

3. EXPERIMENTAL PART:

3.1 Materials:

(±)-Glycidol (96%, sigma-aldrich), *tert*-butyl acetoacetate (TBAA, reagent grade 98%, sigma-aldrich) and 1,3-diaminopropane (DAP, ≥99%, sigma-aldrich) were used as received from Merck. Tris(pentafluorophenyl)borane ($B(C_6F_5)_3$, ›98.0%) was obtained from TCI Europe and purified by sublimation under reduced pressure at 90°C. Toluene (Multisolvent HPLC grade), tetrahydrofurane (THF, multisolvent GPC grade) and diethyl ether (Essent Q, stabilized with approx. 7 ppm of 2,6-Di-tert-butyl-4-methylphenol (BHT)) were purchased from Scharlab, and methanol (MeOH, 99.8% HPLC grade) from Fischer Scientific. All solvents were used as received. Deuterated chloroform (CDCl3, 99.96%, containing 0.03% tetramethylsilane), deuterated water (D2O, 99.9 atom D%) were obtained from Euroisotop. Basic alumina was also purchased from Scharlab.

3.2 Synthesis:

- ### Synthesis of branched cyclic polyglycidol, PG

Polyglycidol was synthesized using glycidol (6.66 g, 6 mL, 90 mmol) as a monomer, toluene (20 mL) as a solvent and $B(C_6F_5)_3$ (59 mg, 0.12 mmol) as a catalyst. The whole reaction was carried out in a jacketed round bottom flask of 100 mL under stirring and argon (Ar) atmosphere. Glycidol and 15 mL of toluene were added into the round bottom flask and cooled down to 0 °C using an ice-bath. Then, the catalyst was dissolved in 5 mL of toluene and added to the reaction at 0 °C under Ar. The polymerization reaction was stirred at 0 °C for 22h. The polymer precipitated during the reaction as a viscous material generating two phases, the solvent and the precipitate. The solvent was removed through decantation. Afterwards, the resulting polymer was dissolved in MeOH (10 mL) and purified by precipitation in diethyl ether (100 mL). Then, the polymer was again dissolved in MeOH (10 mL) and passed through basic alumina. The solvent was removed under vacuum in the rotary evaporator and finally, the isolated product was dried at 80 °C for 18 hours in a vacuum oven. The branched cyclic polyglycidol was obtained as a transparent viscous material (3.31 g, yield 50 %).

- ### Functionalization of polyglycidol with *tert*-butyl acetoacetate, PG-TBAA

PG (250 mg, 3.37 mmol) and a large excess of TBAA (11.18 mL, 67.4 mmol) were added to a schlenk flask of 250 mL with a stir bar. The reaction mixture was stirred at 120 °C for 22h using an oil bath. Then, the reaction mixture was cooled down to r.t and transferred to a round bottom flask of 100 mL. The final product was purified by distillation at 130 °C and 50 mbars for 1 hour to remove the excess of TBAA and the formed *tert*-butanol and afterwards washed with diethyl ether. PG-TBAA was obtained as a viscous yellow oil material (445 mg, 88 % yield).

- General preparation of polymer networks

Several polymer networks containing different amounts of PG-TBAA and 1,3-diaminopropane were prepared. In this section the synthesis of a representative sample is explained:

PG-TBAA (80 mg, 0.53 mmol) was dissolved in THF (9.6 mL) in a 15 mL vial. Separately, in another vial of 10 mL, 1-3 diaminopropane (80 µL, 0.96 mmol) was added to THF (0.96 mL).

Both solutions were stirred for several minutes until complete dissolution. Then, the DAP solution was added to that of the polymer. The mixture was rapidly loaded into a Teflon Petri dish, and the solvent was evaporated at room temperature overnight. The resulting films were further cured at 85 °C for 1 hour under vacuum. Further temperature treatments were evaluated, finally resulting in heating the films at 150 °C for 1 hour under vacuum.

4. CHARACTERIZATION TECHNIQUES:

Several techniques were employed during this work in order to properly characterize all materials including: Fourier Transform Infrared Spectroscopy (FTIR), Differential Scanning Calorimetry (DSC), Thermogravimetric Analysis (TGA), Nuclear Magnetic Resonance (NMR), Gel Permeation Chromatography (GPC) and Elemental Analysis (EA).

4.1 Fourier transform infrared (FTIR) spectroscopy:

The Fourier transform infrared spectroscopy is an analytical technique that studies the interaction between infrared light and molecules, and it is based on the detection of the activities related to molecular symmetry due to changes on the molecular dipoles.

When the infrared radiation beam passes through the sample, the molecules from the sample absorb energy in certain parts of the spectra. This generates different vibrational jumps because of the characteristic vibrational frequencies that each type of chemical bond has, and such vibrational jumps are recorded on the spectrum. Due to the fact that each chemical bond is unique, so it is its vibration frequency and therefore, a unique and unrepeatable fingerprint is observed.

This characteristic makes FTIR a really useful technique for different type of analysis, including the identification of functional groups in the sample. In addition, previously tabulated absorption maxima of several chemical groups facilitate quick identification of specific functional groups, including carbonyls, amides, and alcohols. [17]

In the present work, the FTIR-ATR (Fourier transform infrared spectroscopy – attenuated total reflectance) spectra were taken at room temperature in the spectral region between 600-4000 cm^{-1} on a JASCO 3600 FTIR spectrometer equipped with an ATR accessory (**Figure 8**). Each sample was analysed with a 4 cm^{-1} resolution and an average of 200 scans. The spectrum baseline was not corrected, nor was the spectrum smoothed.

Figure 8: Employed JASCO 3600 FTIR spectrometer.

4.2 Differential Scanning Calorimetry (DSC):

DSC is an analytical technique that studies the thermal properties/behaviour of materials. DSC works by comparing the sample to be analysed and a reference under equal thermal conditions. A thermogram is obtained where heat flow is represented in function of temperature or time. The thermal events that can be detected are associated to physical or chemical changes occurring in the sample. Among them, endothermic processes such as evaporation or melting, as well as exothermic processes including crystallization and chemical reactions can be recorded. For instance, melting and crystallization temperatures, melting and crystallization enthalpies and glass transition temperatures (Tg) can be recorded. [18]

In the present work, DSC was performed in a Q2000 TA Instruments. Samples of approximately 5 mg were encapsulated in in aluminium pans and the scans were carried out at 10 °C/min heating and cooling rate, with a Helium flow of 25 mL/min. The following thermal protocol was followed:

1) Ramp from 40 °C to -100 °C at 10 °C/min
2) Ramp from -100 °C to 150 °C at 10 °C/min (first scan)
3) Ramp from 150 °C to -100 °C at 10 °C/min
4) Ramp from -100 °C to 150 °C at 10 °C/min (second scan)
5) Ramp from 150 °C to -100 °C at 10 °C/min
6) Ramp from -100 °C to 150 °C at 10 °C/min (third scan)

For those samples in which the Tg could not be well detected below 150 °C, the third cycle was heated to 220 °C and a subsequent cooling and heating cycles were performed to ensure the thermal stability of the sample.

4.3 Thermogravimetric Analysis (TGA):

TGA is a thermal analysis technique that studies thermal stability of materials by measuring mass changes in function of time and/or temperature under well-controlled atmosphere, for example inert or oxidant atmosphere. The mass changes can be due to decomposition, dehydration or oxidation.

TGA was carried out in a TGA Q500 TA Instruments **(Figure 9)**, under nitrogen atmosphere (constant flow of 60 mL/min). Samples were heated from 25 °C to 600 °C with a heating ramp of 10 °C/min.

Figure 9: Q500 TA INSTRUMENTS equipment for thermogravimetric analysis.

4.4 Nuclear Magnetic Resonance (NMR):

NMR is an analytical technique employed to determine molecular structure and chemical compositions of samples. Such technique is based on the interaction between spinning nuclei in a magnetic field with a selective range of radiofrequency.
The magnetic active nuclei are randomly oriented in absence of a magnetic field. When the sample is submitted to a magnetic field, the nuclei with positive spin are oriented

in the same direction as the magnetic field, (alpha state) and the nuclei with negative spin are oriented in the opposite way (beta state). The alpha spin represents lower energy state whereas beta spin represents a higher energy state. In this way, once the samples have been submitted and afterwards removed from the magnetic field, the emitted frequency signals depend on the energy difference between both states, giving raise to the spectrum from where the structures are studied.

In this work, ^{1}H NMR spectra were acquired in a Bruker Advanced Neo Instrument at 400 MHz and room temperature, employing deuterated water (D_2O) for PG and deuterated chloroform ($CDCl_3$) for PG-TBAA.

4.5 Gel Permeation Chromatography (GPC):

GPC also known as Size Exclusion Chromatography (SEC), is a characterization technique commonly used to measure molecular masses (M_n, M_w...) of polymers and molecular weight distributions including dispersity index (Đ). It is based on the separation of macromolecules depending on their hydrodynamic volume or size.

GPC technique involves the use of a column filled with porous beads as the stationary phase, where the size of these pores is variable. Because of this, small molecules are able to penetrate the pores and spend longer times inside the column, resulting in longer elution times. On the other hand, larger molecules which are not able to enter the pores move freely and spend less time inside the column, resulting in shorter elution times. [19]

Detectors such as differential refractometer (dRI) or Ultraviolet (UV) absorption detectors monitor the elution of the mentioned molecules. A calibration curve using polymer standards relate the retention time of the measured polymer with the molecular weight of the polymer standard (e.g. polystyrene, polyethylene...). In this case, relative molecular weights of the polymer are determined. By using an additional detector, multiangle light scattering (MALS), absolute molecular mass can be obtained if the specific refractive index increment (dn/dc) of the polymer is known.
The GPC measurements for this project were performed on a Shimadzu Nexera 40 HPLC system (**Figure 10**), equipped with a polar gel-M guard (50x7.5 mm) and a polar

gel-M column (300x7.5 mm), both from Agilent. A differential refractive index (dRI) detector (RID-20A, Shimadzu) and a multiangle light scattering (MALS) detector (MiniDawn, Wyatt) were used as a double detection system. Data analysis was performed with ASTRA Software from Wyatt. The eluent used was DMF with 0.1% of LiBr, at a flow rate of 1 mL/min and an oven temperature of 50 °C. A dn/dc value for polyglycidol of 0.054 mL/g was used. [20]

Figure 10: Shimadzu Nexera 40 HPLC system employed in this work.

4.6 Elemental Analysis (EA):

EA is an analytical technique employed to determine the chemical composition of samples. Even there are different techniques employed, one of the most common ones is CHNS (Carbon-Hydrogen-Nitrogen-Sulfur) analysis which is focused on determining the amount of such elements in the sample.

This technique involves pyrolysis of the sample followed by detection and quantification of the resulting combustion products. Oxygen is then determined as the difference between the total percentage and the obtained amount of CHNS. [21]

In the present work, elemental analysis was performed in an Elemental Analyzer EuroEA 3000 (Eurovector, Italia).

5. RESULTS AND DISCUSSIONS:

5.1 Synthesis and characterization of branched cyclic polyglycidol:

Polyglycidol (PG) was obtained by means of ZROP using $B(C_6F_5)_3$ as a catalyst in toluene, as it is described by Kim's group in the reference [18] (**Figure 11**).

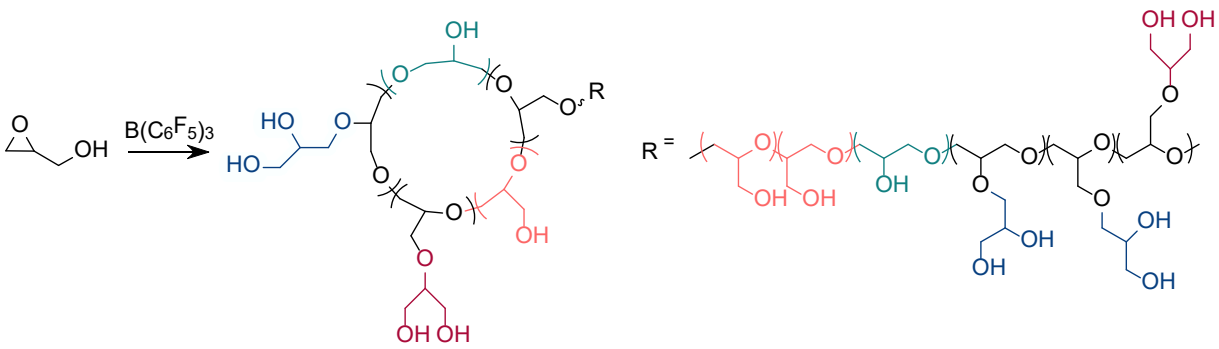

Figure 11: Scheme of the cationic ring-opening polymerization of the glycidol monomer.

The synthesis of branched cyclic polyglycidol was confirmed by ^{1}H and ^{13}C NMR.

^{1}H NMR spectra, as shown in **Figure 12,** was used to calculate the monomer conversion of the product by comparing between the glycidol and the crude polyglycidol ^{1}H spectra. Signals were assigned and integrated and the conversion (P) was calculated by using

Equation *1* where I_B is the integrated area of the signal B in the polyglycidol spectrum and I_A is the integrated area of signal A, which includes the signals d, c, b of the polymer and signals D and C of the monomer.

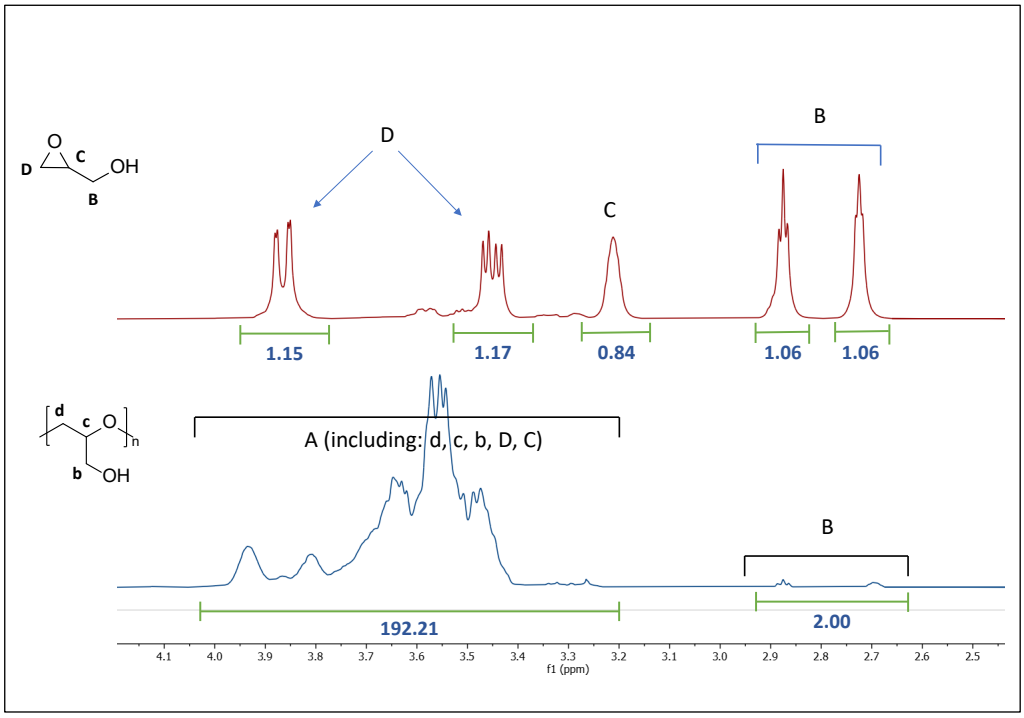

Figure 12: Glycidol and crude polyglycidol ^{1}H RMN spectra using D_2O.

$$P(\%) = \left(1 - \frac{\frac{I_B}{2}}{\frac{I_B}{2} + \left(\frac{I_A - \frac{I_B}{2} \times 3}{5}\right)}\right) \times 100$$

Equation 1

In this way, a monomer conversion of 98.6% was calculated, confirming the high catalytic activity of $B(C_6F_5)_3$ in this type of reactions. To evaluate the degree of branching (DB) of PG, ^{13}C NMR signals were assigned according to references [8, 22], as shown in **Figure 13**.

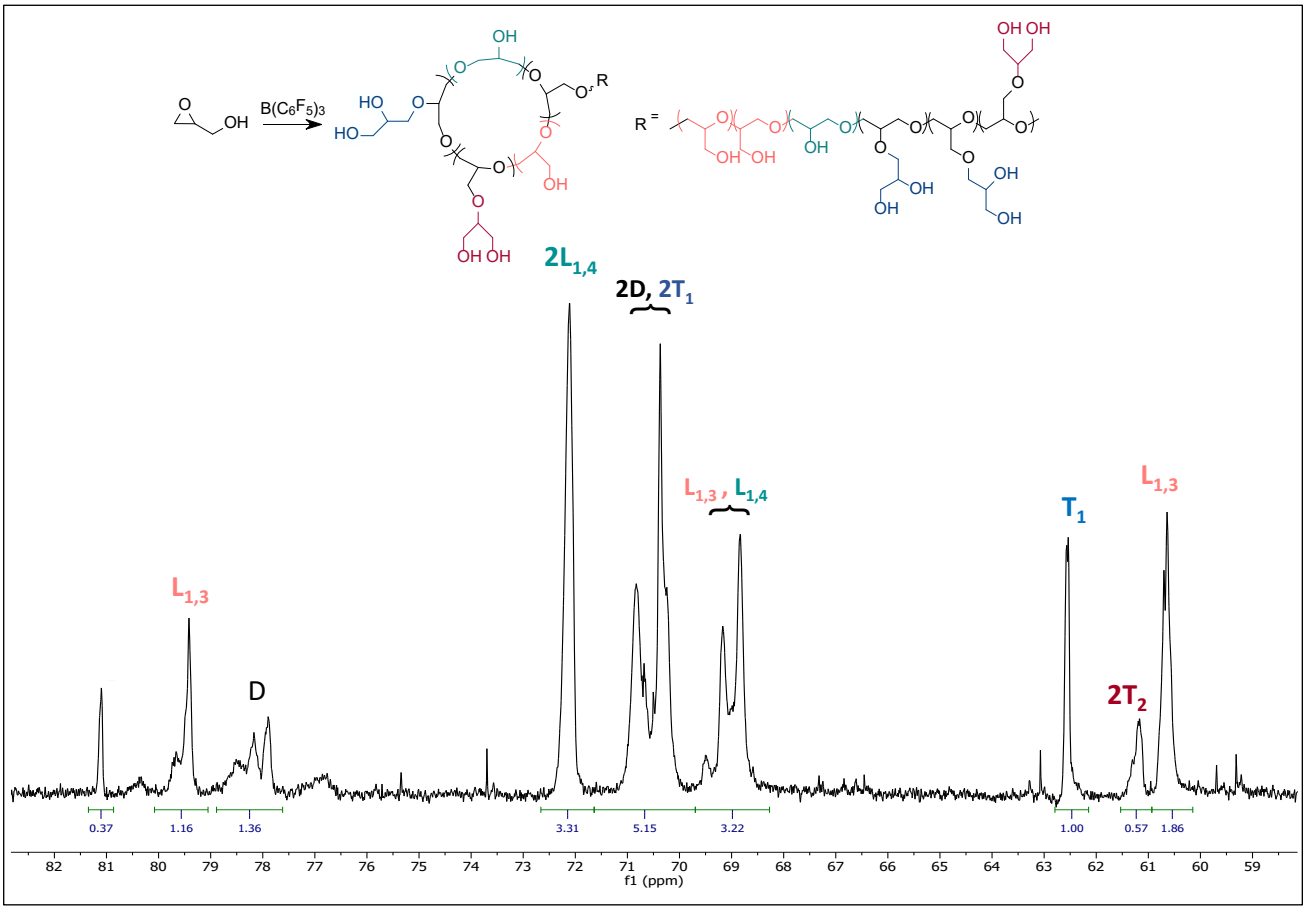

Figure 13: Structural analysis of inverse-gated ^{13}C NMR spectra of polyglycidol using D_2O.

Once the assignment of signals was done, the DB was calculated from **Equation 2** where D, $L_{1,3}$ and $L_{1,4}$ are the relative abundances of dendritic and linear structures. [18] The obtained value for DB for PG was of 0.48, in agreement with the data previously obtained. [8]

$$DB = \frac{2D}{2D + L_{1,4} + L_{1,3}}$$ **Equation 2**

The characterization of PG with GPC showed a number average molecular weight (M_n) of 10.1 kDa and a dispersity index (Đ) of 1.7.

Universidad del País Vasco Euskal Herriko Unibertsitatea

5.2 Characterization of functionalized PG-TBAA:

Functionalization of PG was achieved by the transesterification reaction of PG with TBAA (**Figure 15**). Once the removal of excess of TBAA and formed *tert*-butanol was confirmed, quantification of the amounts of TBAA groups in PG-TBAA was done. First, identification of ^{1}H NMR signals (**Figure 14**) was performed with the help of HSQC and DEPT 135° experiments (**Figure 16**).

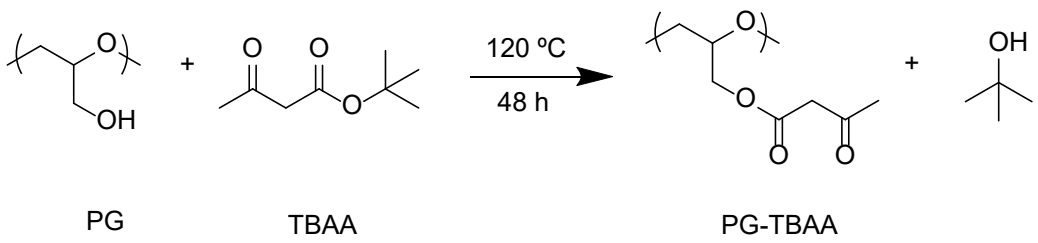

Figure 15: Functionalization reaction of PG.

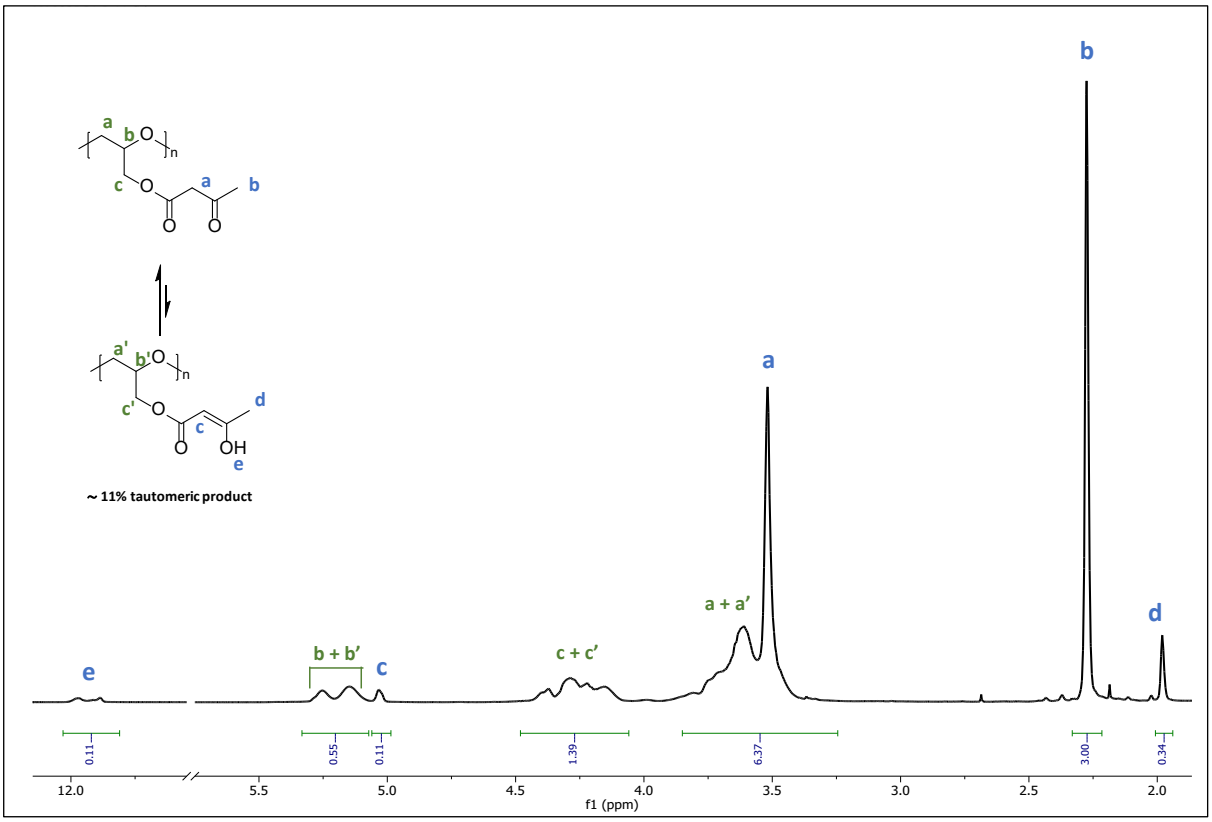

Figure 14: 1H RMN spectrum of PG-TBAA using $CDCl_3$.

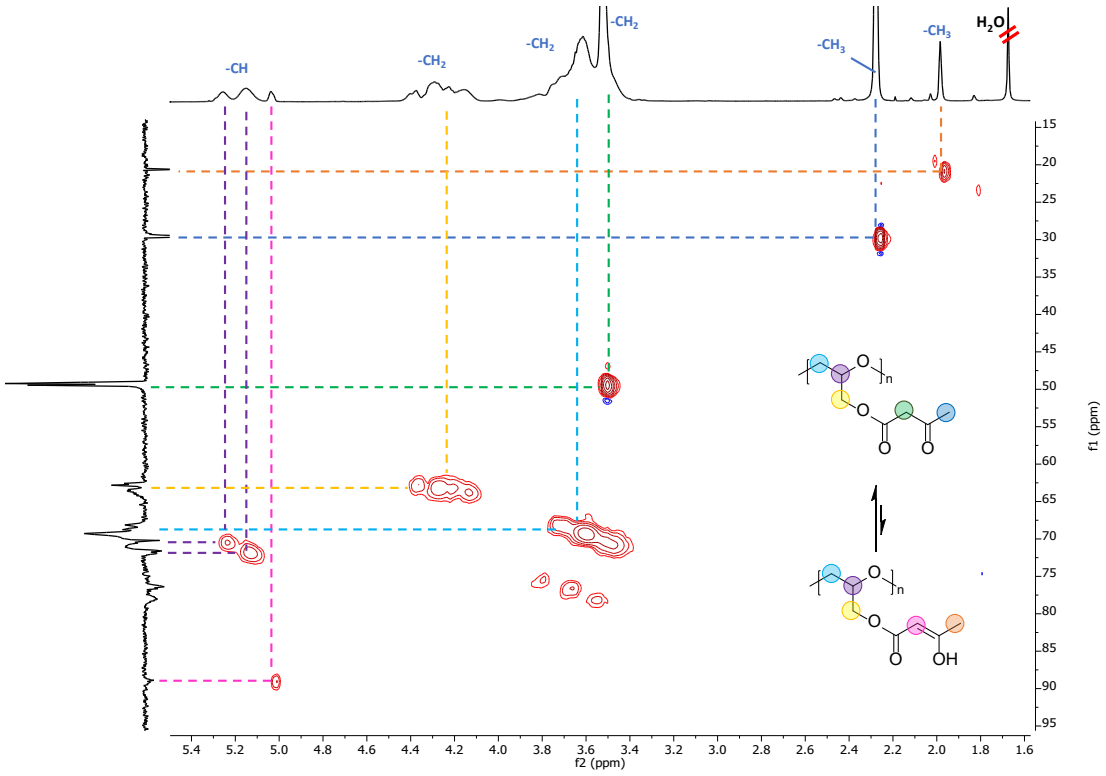

Figure 16: HSQC spectrum of PG-TBAA. DEPT 135° in the vertical trace is shown.

In the previous figure (**Figure 16**), the HSQC spectrum was represented showing the DEPT 135° in vertical trace, in which ^{13}C signals arising due to methyl ($-CH_3$) and methine (-CH) appear negative, methyne ($-CH_2$) as positive and no quaternary carbons show up. In this way, the different type of signals were easily distinguished and correlated to those appearing in the HSQC, as show the straight lines on the figure, each of it corresponding to a different type of bond, allowing a complete characterization of the structure.

Protons corresponding to the enol form of the ß-ketoester were detected at δ =1.98, 5.05 and 11.85 ppm in the ^1H-NMR spectra showing the occurrence of keto–enol tautomerism in solution. Comparison of the peak integrals of $-CH_3$ of both the keto and the enol forms (δ = 2.28 ppm and 1.99 ppm, respectively) indicated that 88 % existed in the keto form.

Considering the tautomerism of the obtained product, functionalization of TBAA was calculated by comparison of the signals corresponding to the polymer and the signals corresponding to the TBAA.

Following **Equation 3**, a functionalization of 88 % was calculated. For that, the integrated area corresponding to the sum of both keto and enol forms of a well-known peak of the TBAA structure, as it is the methyl, was divided by the integrated area of the keto and enol forms corresponding to the polymer signals.

$$\text{Functionalization } (\%) = \frac{\left(\frac{b}{3}+\frac{d}{3}\right)}{\frac{(b+b')+(c+c')+(a+a')}{5}} \times 100 \qquad \textbf{Equation 3}$$

The formation of the functionalized product was also confirmed by TGA, FTIR and DSC.

By TGA analysis, changes on the thermal stability of the new product compared to PG were proved. As it is shown in **Figure 17**, PG is thermally stable up to ~ 330 °C despite having a slight weight loss of ~ 8% at around ~ 100 °C attributed to the evaporation of remaining solvents and water of hydration. The onset temperature was calculated by linear extrapolation obtaining a value of 375 °C.

Regarding PG-TBAA, it is observed that after the functionalization the thermal stability decreases, being the onset temperature 235 °C. This decrease likely occurs because of the incorporation of less thermally stable carbonyl groups into the polymer structure. A weight loss of ~ 40 % at around 300 °C attributed to the degradation of the TBAA groups in the sample clearly occurs prior to the degradation of the polymer backbone.

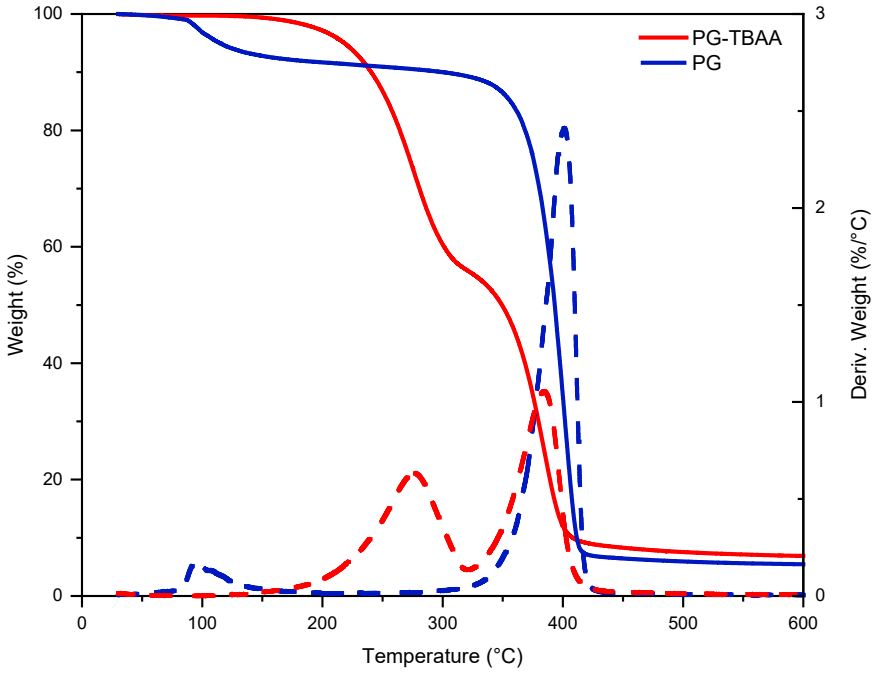

Figure 17: TGA measurements of PG and PG-TBAA.

Then, by means of FTIR spectroscopy, functionalization of PG with TBAA was proved, as shown in **Figure 18**.

ATR-FTIR spectrum of PG showed a broad absorption band at approximately 3300 cm^{-1} corresponding to the O-H stretching vibrations (ν_{OH}) of the hydroxyl groups, while in functionalized PG there was a visible decrease in such band, since the majority of the hydroxyl groups reacted to form ester groups. Note that the remaining intensity of the peak could be due to the contribution of ν_{OH} of H_2O whose signals also appear in this region.

The appearance of ß-ketoester groups was proved from the appearance of a strong double peak appearing at 1745 and 1715 cm^{-1} corresponding to the C=O stretching vibrations of the ester and the ketone groups, respectively.

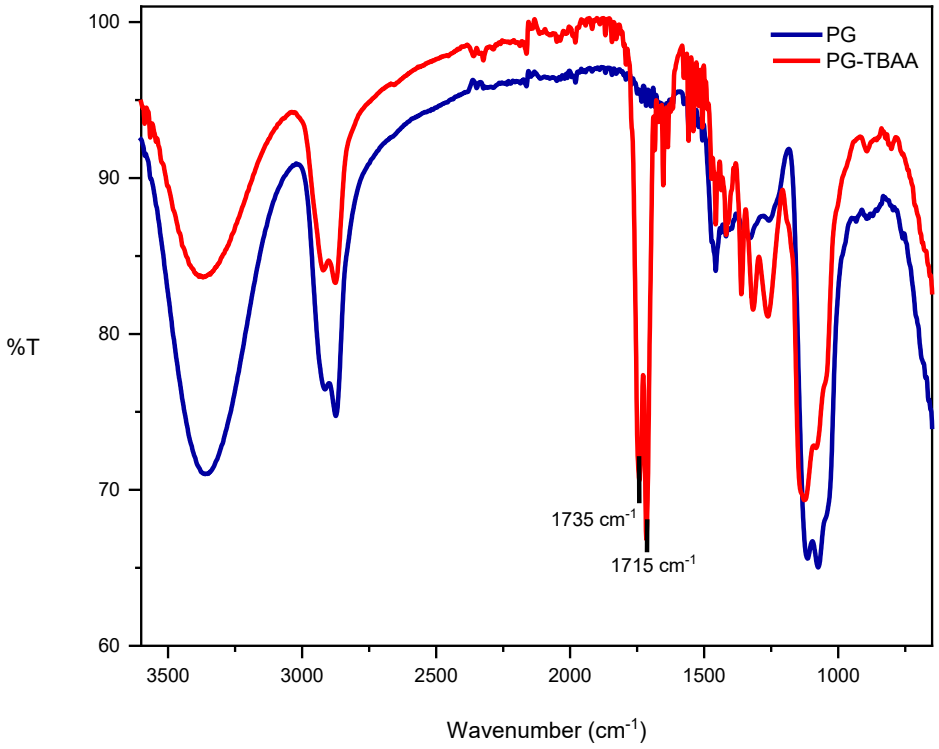

Figure 18: Comparative FTIR spectra of PG and PG-TBAA. The spectra were vertically shifted.

By DSC, as shown in **Figure 19**, the Tg value of PG was found to be -11 °C. It has to be mentioned that previous experiments on moisture absorption had shown the great influence of a drying process, since the sample is very hygroscopic. Removal of water was necessary in order to achieve a reliable value. Therefore, the sample was firstly heated up to 150 °C in a first heating run at 10 °C/min, where a broad endotherm appeared because of water evaporation. Then, the value of Tg represented is that one obtained in the second heating run.

DSC analysis of PG-TBAA showed a Tg value of -24 °C, which is lower than that of PG. This can be due to the suppression of hydrogen bonds in PG upon functionalization. [23]

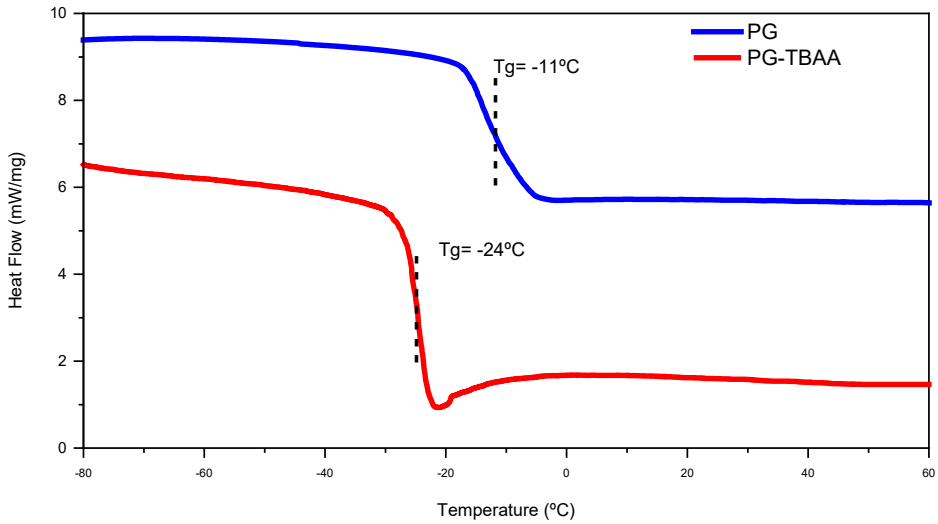

Figure 19: Differential scanning calorimetry (DSC) plots showing medium Tg values of PG and PG-TBAA.

5.3 Synthesis and characterization of crosslinked networks:

Several crosslinked networks were synthetized by varying the equivalents of the 1,3-diaminopropane relative to the amounts of TBAA groups in PG-TBAA, as reported in **Table 1**:

Table 1: Amounts of 1,3-diaminopropane relative to the amounts of TBAA groups in PG-TBAA.

Name	mol DAP / mol of TBAA in PG-TBAA
R-0.3	0.3
R-0.4	0.4
R-0.5	0.5
R-0.6	0.6
R-0.7	0.7
R-0.8	0.8
R-1	1
R-1.5	1.5
R-2	2
R-4	4

The crosslinking reaction is thermally activated with a concomitant loss of water, as shown in **Figure 20**.

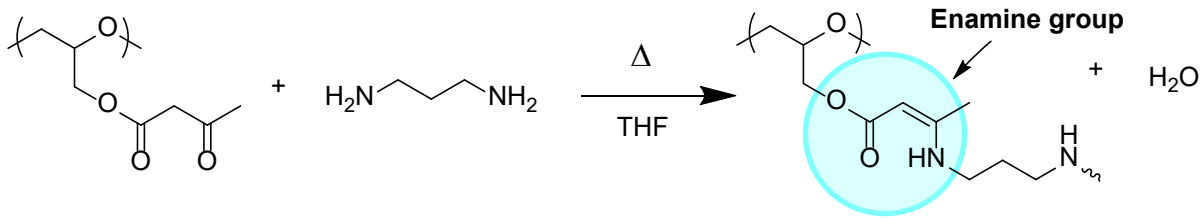

Figure 20: Crosslinking reaction of PG-TBAA with DAP.

In order to evaluate the thermal treatment to be used in all samples we first analyzed by TGA a representative sample (R-2) that was subjected to different thermal protocols:

(1) As obtained, without any thermal treatment.
(2) After being heated at 85 °C for 7 hours.
(3) After being heated at 150 °C for 1 hour.

The need of a thermal treatment was clear as observed in **Figure 21**. The network that had not undergone a thermal treatment **(1)** has a weight loss of nearly 57 % up to 170 °C which can be attributed to the loss of water upon reaction and free DAP. This is supported by the fact that DAP has a boiling temperature of ~ 140 °C. These results indicated that the formation of PG-based crosslinked networks had to be followed by a thermal treatment that allowed water evaporation and free DAP removal. We first tried by heating the sample at 85 °C for 7 h **(2)**. However, the sample still exhibited a weight loss at around ~ 150 °C, which could be from residual free DAP. This suggested that a thermal treatment with higher temperature was needed. Then, we heated the sample at 150 °C for 1 h **(3)**. TGA data showed a much thermally stable sample with an onset decomposition temperature at ~ 318 °C. It has to be mentioned that upon heating at 150 °C the sample did not exhibit colour change, which was indicative of thermal stability.

It is clearly seen that the most adequate treatment is the one of 1h at 150 °C because apart from being faster it is also more efficient. For instance, the 8 % weight loss at 200 °C observed in treatment **(3)** is avoided probably because the free DAP was eliminated during the vacuum heating. For that reason, the thermal treatment at 150 °C was used in the rest of the samples by varying the heating time according to the TGA profile of unheated sample (from 15 min to 1 h).

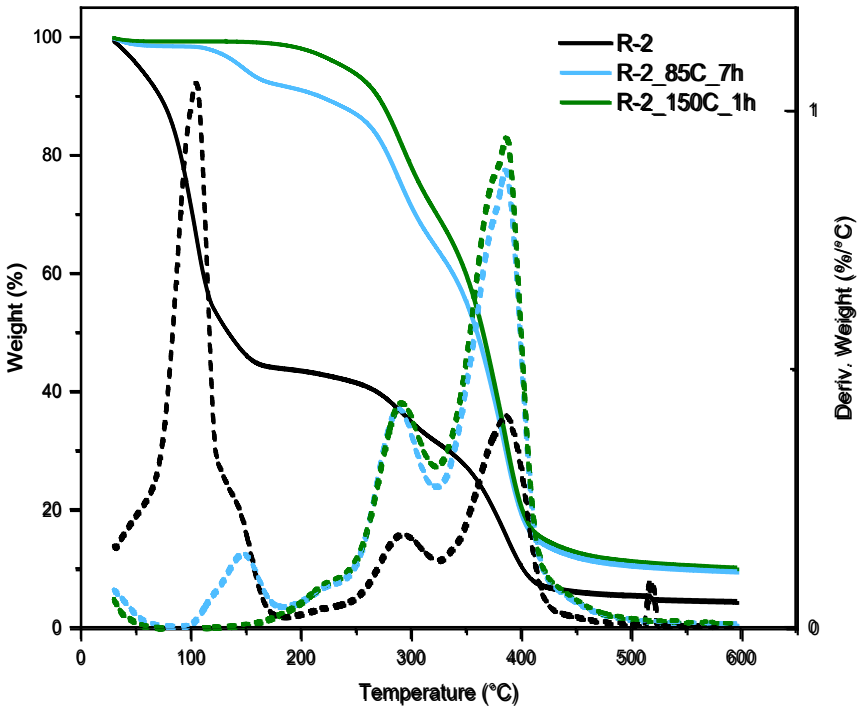

Figure 21: TGA data of R-2 samples.

Differences between the 3 thermally treated samples were also confirmed by FTIR spectroscopy, as shown in **Figure 22**.

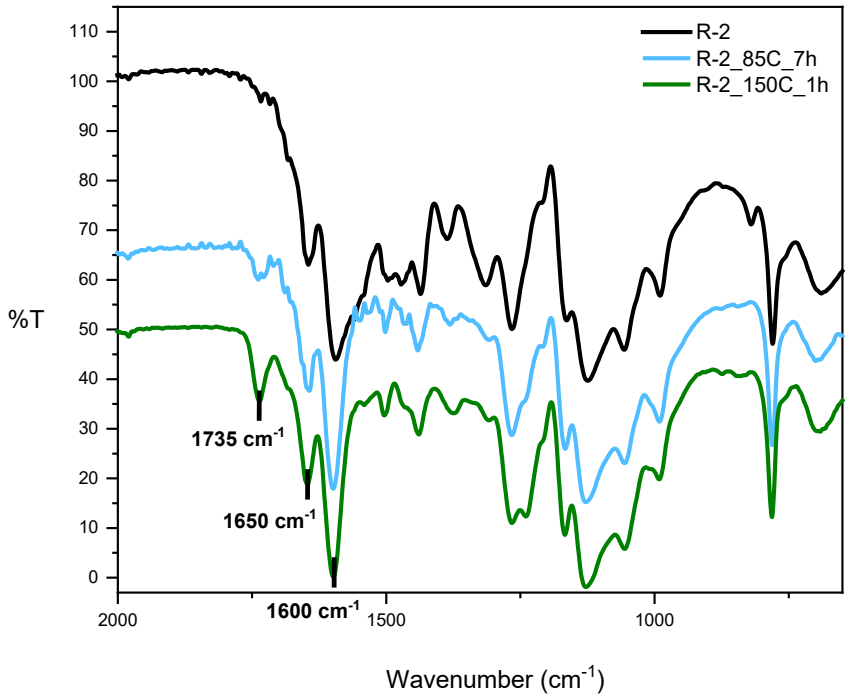

Figure 22: Comparative FTIR spectra of R-2 samples with different treatments.

Once again, it is possible to observe the suitability of the treatments at 85 °C and 150 °C. The appearance of a well-defined peak at 1735 cm^{-1} corresponding to the formation of the C=O bond that is not seen in the unheated sample, evidences the formation of the ester group. In addition, the peaks around 1650 and 1600 cm^{-1} corresponding to the δ_{N-H} and the $\nu_{C=C}$ bonds respectively, confirm the formation of the enamine group (**Figure 20**). [11]

Once the heat treatment to be carried out was defined, all of the synthetized films **Table 1** were thermally treated and afterwards their characterization was performed by TGA, FTIR and DSC.

TGA results of several samples are shown in **Figure 23**. It is clearly observed that as DAP amount increases, more stable the samples are, reaching an onset degradation temperature around 200 °C in the great majority of the samples. In the case of the

sample with less amount of DAP (R-0.3) the onset degradation temperature occurs ~ 20 °C below than in the rest of the samples. This is possibly due to the fact that not all the TBAA groups have been reacted with DAP and therefore the remaining TBAA groups start the degradation process at lower temperatures than those that have formed an enamine group. In this sense, it is likely that the degradation step starting at ~ 250 °C can be attributed to formed enamine groups.

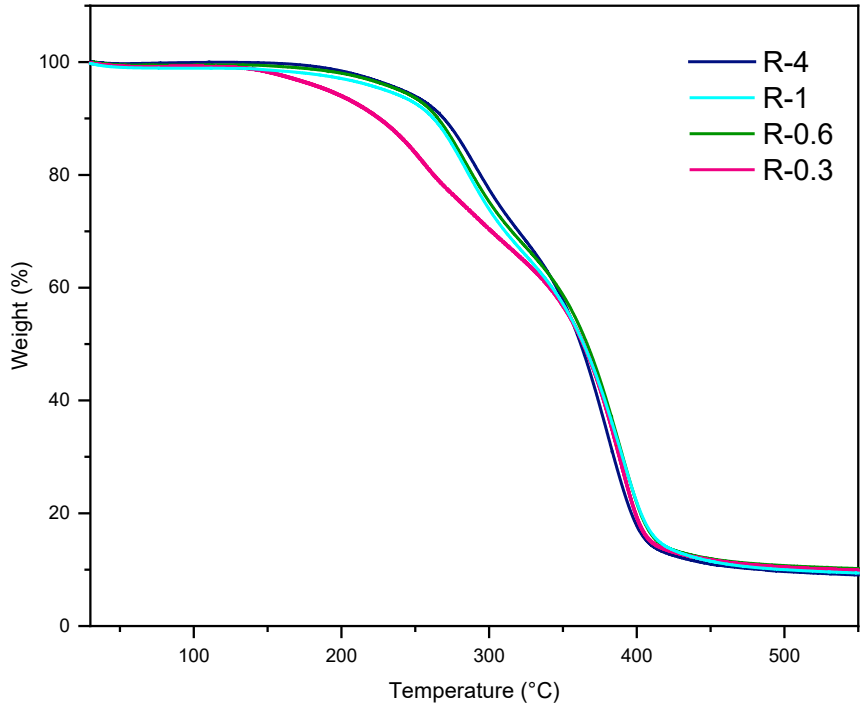

Figure 23: TGA data of several polymer networks.

In **Figure 24**, the FTIR/ATR analysis of all synthetized films after applying the aforementioned thermal treatment is shown.

As well as in the previous figure, the formation of the enamine is verified by the peaks appearing around 1650 and 1600 cm^{-1} corresponding to the δ_{N-H} and the $\nu_{C=C}$ bonds, respectively. In addition, it is observed that those samples with less amount of DAP still have the double peak around 1745 and 1715 cm^{-1} corresponding to the C=O stretching vibrations of the ester and the ketone groups respectively, because of the still

remaining TBAA groups in the samples. Nevertheless, as the amounts of DAP increase and so the TBAA groups in the samples decrease, the just mentioned double peak disappears giving way to a single peak at 1735 cm^{-1} corresponding to the C=O of the ester group belonging to the enamine.

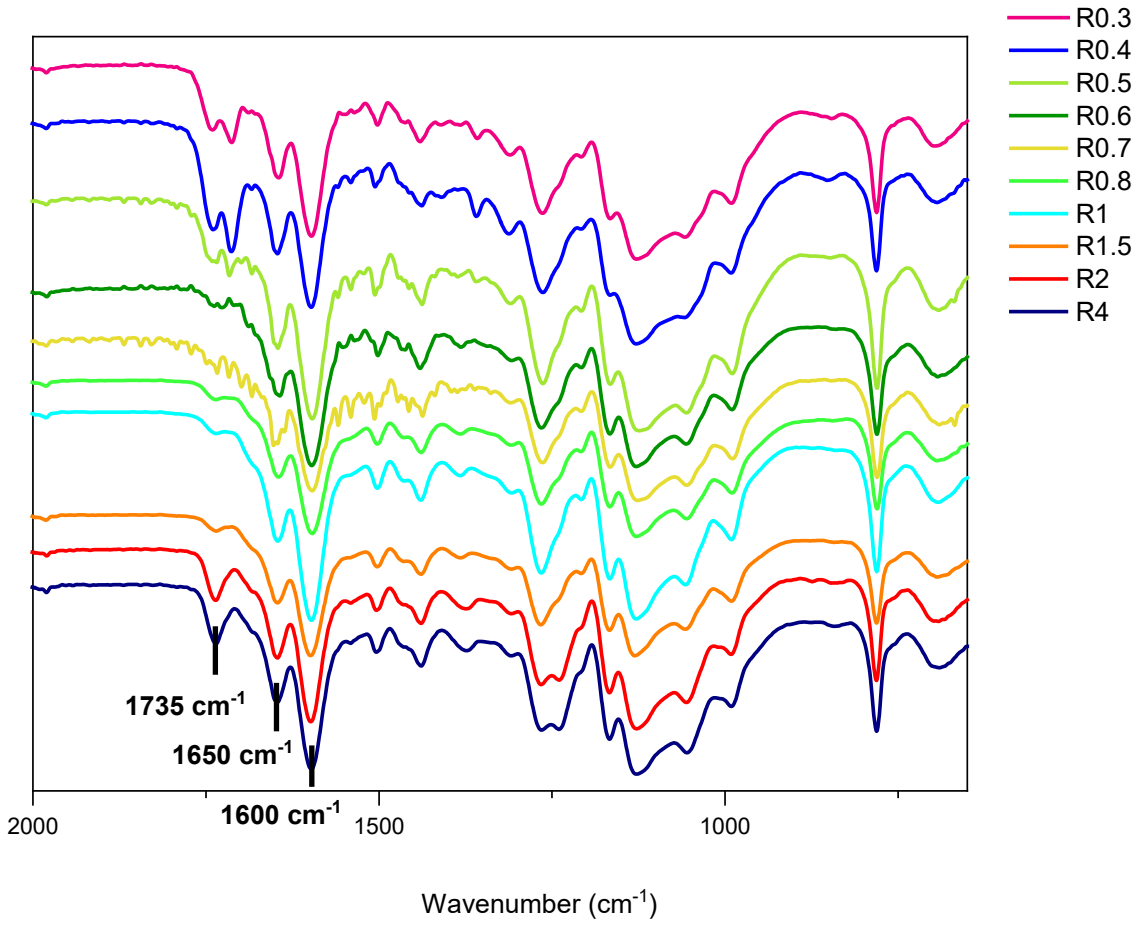

Figure 24: Comparative FTIR spectra of the films.

In order to determine the amount of nitrogen in the samples, elemental analysis was carried out. The obtained results are summarized in the following table (**Table 2**):

Table 2: Elemental analysis of the films.

Name	C/(wt%)	H/(wt%)	N/(wt%)	O calculated/(wt%)
R-0.3	56.26	6.50	4.37	32.87
R-0.4	54.60	6.32	3.84	35.24
R-0.5	55.73	7.49	6.19	30.59
R-0.6	56.02	7.56	7.96	28.46
R-0.7	56.17	7.55	7.78	28.5
R-2	55.01	6.24	6.36	32.39
R-4	56.67	7.02	6.66	29.65

As it is observed in the table, when the amount of DAP increases, the nitrogen percent also increases in the samples until reaching a maximum where the crosslinking is probably complete. The theorical amount of nitrogen if all of the TBAA groups have reacted was calculated (**Equation 4**). This was done by dividing the theorical % of nitrogen in one monomer unit of the crosslinked network (taking into account the previously obtained functionalization, **Equation 3**) by the sum of the total molecular masses, also considering the functionalization of each form. A maximum of 7.2 % amount of nitrogen is expected. This means that those samples that have higher percentage of nitrogen (R-0.6 and R-0.7) probably have amine dangling chains on their structure.

$$\mathrm{N}\ (\%) = \frac{m_N \times 0.88}{(m_{(C_3H_6O_2)} \times 0.12) \times (m_{(C_9H_{15}O_3N)} \times 0.88)} \qquad \textbf{Equation 4}$$

The Tg values of the films ranged from 18 °C to 100 °C passing through a maximum at 140 °C, as shown in **Figure 25**. The results indicated that the Tg was influenced by the amount of diamine present in the samples.

As it is observed, the Tg increases with the amount of DAP due to an increase in the number of crosslinks, which provide chain rigidity. The maximum Tg is achieved with (0.8 mol of DAP per TBAA units), which is slightly higher than that expected for obtaining a maximum number of crosslinks (0.5 mol /TBAA). This means that not all the TBAA units are accessible to DAP, and therefore, an excess of the diamine is required to reach the maximum number of crosslinks. A high excess of DAP likely results in dangling amine chains, thereby reducing the Tg and reaching a plateau at around 100 °C.

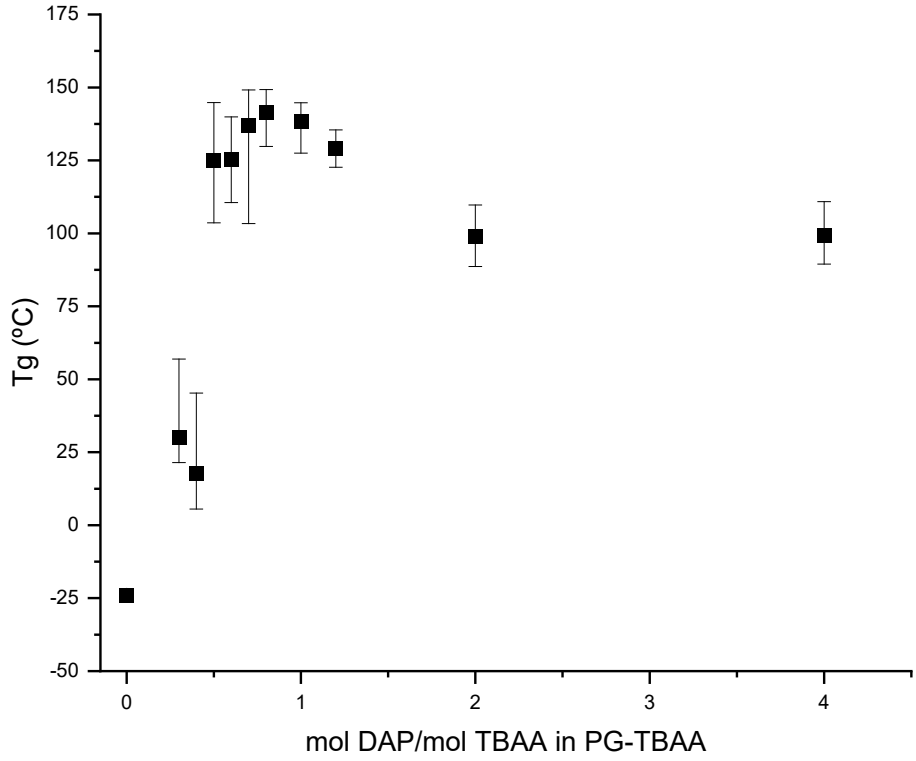

Figure 25: Medium Tg data of PG-based CN. The bars represent the onset and end points of the glass transitions.

Finally, in order to test the enamine's bond ability to exchange with other amines, samples were exposed to an excess of monofunctional amine. In this sense, several representative samples were submerged in propylamine for 24 hours, and afterwards 1 mL of THF was added. The exchange reaction occurred efficiently with help of high temperature (**Figure 26-1**).

Universidad del País Vasco Euskal Herriko Unibertsitatea

Additionally, in order to demonstrate the pH-responsiveness of the crosslinked networks, phosphoric acid (H_3PO_4) was added. Again, several representative samples were submerged in H_3PO_4 for 24 h and afterwards 1 mL of THF was added. After 96 h complete degradation was observed (**Figure 26-2**), which suggests that these types of materials can be efficiently disassembled, enabling easy management at the end of their life cycle and the possibility of chemical recycling.

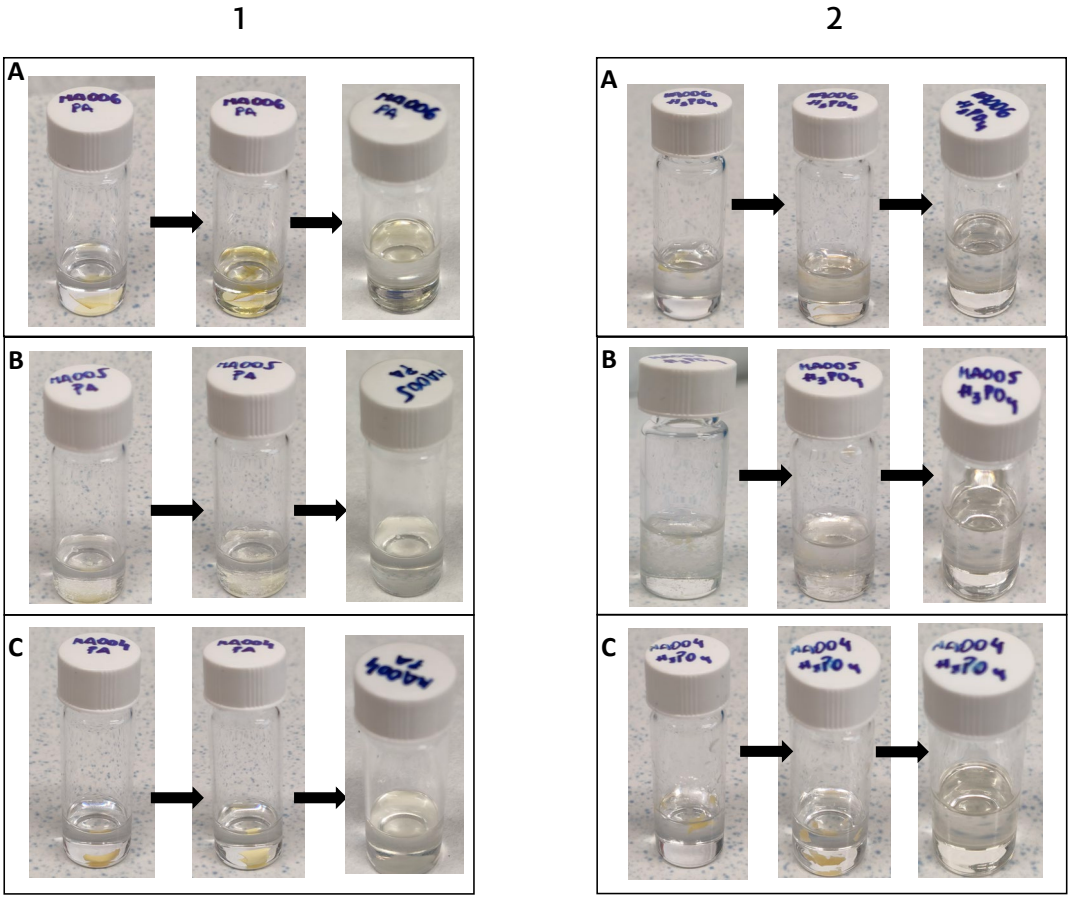

Figure 26: (1) Crosslinked networks showing enamine's bond ability to exchange with amines. (1A, 1B, 1C) R-0.3, R-0.6, R-2, respectively, immersed in 1 mL of propylamine (i), followed by 1 mL of THF after 24 hours and (ii) heating 70°C for 24 hours. (2) pH-responsiveness of crosslinked networks. (2A, 2B, 2C) R-0.3, R-0.6, R-2, respectively, dissolved in 1 mL of H3PO4, (i), followed by 1 mL of THF after 24 hours and complete degradation after 96 hours.

6. CONCLUSIONS

Throughout this work, synthesis and characterization of polyglycidol-based crosslinked networks was carried out. To this aim, polyglycidol was first synthetized by ZROP of glycidol with $B(C_6F_5)_3$.

Functionalization of polyglycidol was successfully conducted by transesterification of OH groups of polyglycidol with *tert*-butyl acetoacetate and corroborated with RMN techniques (^1H, HSQC, DEPT 135°). The formation of the ß-ketoester groups was confirmed by FTIR technique.

The synthesis of the crosslinked networks was carried out employing 1,3-diaminopropane, with increasing number of equivalents related to the amount of the TBAA functional groups.

Crosslinked polyglycidol with enamine bonds was successfully obtained, whose Tg depends on the degree of crosslinking of the sample. In addition, the ability of the enamine bond to exchange with other amines as well as pH-responsiveness of the crosslinked networks was proved.

This study lays the groundwork for future research on the formation of crosslinked networks of PG with enamine bonds, and for the tuning of the Tg of these materials.

REFERENCES

1. Ebewele, R. O. *Polymer science and technology*. (CRC press, 2000).
2. Nuyken, O. *et al. Ring-opening polymerization—an introductory review*. vol. 5(2), 361-403 (Polymers, 2013).
3. Odian, G. *Principles of polymerization*. (John Wiley & Sons, 2004).
4. Bochenek, M. *et al.* Polyglycidol of Linear or Branched Architecture Immobilized on a Solid Support for Biomedical Applications. *Polymer Reviews* **60**, 717–767 (2020).
5. Du, Y. *et al.* Tunable Multicolor Luminescence Polyglycidol-Acrylates: One-Pot Preparation and Properties. *ACS Appl Polym Mater* **5**, 3817–3826 (2023).
6. Brown, H. A. *et al.* Zwitterionic ring-opening polymerization for the synthesis of high molecular weight cyclic polymers. *Acc Chem Res* **46**, 2585–2596 (2013).
7. Ochs, J. *et al.* Macrocyclic polymers: Synthesis, purification, properties and applications. *Prog Polym Sci* **134**, 101606 (2022).
8. Al Assiri, M. A. *et al.* Reactivity of B(C6F5)3 towards glycidol: The formation of branched cyclic polyglycidol structures. *Eur Polym J* **171**, 111194 (2022).
9. Gu, Y. *et al.* Polymer networks: from plastics and gels to porous frameworks. *Angewandte Chemie International Edition* **59**, 5022–5049 (2020).
10. Lucherelli, M. A. *et al.* Combining Associative and Dissociative Dynamic Linkages in Covalent Adaptable Networks from Biobased 2,5-Furandicarboxaldehyde. *ACS Sustain Chem Eng* **11**, 2334–2344 (2023).
11. Stewart, K. A. *et al.* Dynamic Ablative Networks: Shapeable Heat-Shielding Materials. *ACS Appl Mater Interfaces* **15**, 25212–25223 (2023).
12. Lagron, A. B. *et al.* Characterization Techniques to Assess Recyclability in Dynamic Polymer Networks. *Front Mater* **9**, (2022).
13. West, J. A. The chemistry of enamines. *J. Chem. Educ.* 40–194 (1963).
14. Sánchez, D. *et al.* Relative Tendency of Carbonyl Compounds To Form Enamines. *Org Lett* **14**, 536–539 (2012).

15. Maeda, T., Otsuka, H. & Takahara, A. Dynamic covalent polymers: Reorganizable polymers with dynamic covalent bonds. *Prog Polym Sci* **34**, 581–604 (2009).
16. Sanchez-Sanchez, A., Fulton, D. A. & Pomposo, J. A. pH-responsive single-chain polymer nanoparticles utilising dynamic covalent enamine bonds. *Chemical Communications* **50**, 1871–1874 (2014).
17. Danielsen, S. P. O. *et al.* Molecular Characterization of Polymer Networks. *Chem Rev* **121**, 5042–5092 (2021).
18. Schick, C. Differential scanning calorimetry (DSC) of semicrystalline polymers. *Anal Bioanal Chem* **395**, 1589–1611 (2009).
19. Trathnigg, B. Size-exclusion chromatography of polymers. *Encyclopedia of analytical chemistry* 8008–8034 (2000).
20. Utrata-Wesołek, A. *et al.* Modified polyglycidol based nanolayers of switchable philicity and their interactions with skin cells. *Eur Polym J* **49**, 106–117 (2013).
21. Frąckowiak, E. *et al.* Chapter Five - Advanced characterization techniques for electrochemical capacitors. in *Advances in Inorganic Chemistry* (eds. van Eldik, R. & Hubbard, C. D.) vol. 79 151–207 (Academic Press, 2022).
22. Kim, S. E. *et al.* A recyclablemetal-free catalytic system for the cationic ring-opening polymerization of glycidol under ambient conditions. *Green Chemistry* **24**, 251–258 (2022).
23. Schubert, C. *et al.* Can Hyperbranched Polymers Entangle? Effect of Hydrogen Bonding on Entanglement Transition and Thermorheological Properties of Hyperbranched Polyglycerol Melts. *Macromolecules* **49**, 8722–8737 (2016).